

SNF2H interacts with XRCC1 and is involved in repair of H₂O₂-induced DNA damage

Yoshiko Kubota*, Shinji Shimizu, Shinji Yasuhira and Saburo Horiuchi

Department of Molecular Biochemistry, Department of Tumor Biology, School of Medicine, Iwate Medical University, 2-1-1 Nishitokuta, Yahaba, Shiwa, Iwate, 028-3694, Japan

* To whom correspondence should be addressed. Email, yoshikok@iwate-med.ac.jp; Tel, +81 19 651 5111; Fax, +81 19 907 1904. Department of Molecular Biochemistry, School of Medicine, Iwate Medical University, 2-1-1 Nishitokuta, Yahaba, Shiwa, Iwate, 028-3694, Japan.

ABSTRACT

The protein XRCC1 has no inherent enzymatic activity, and is believed to function in base excision repair as a dedicated scaffold component that coordinates other DNA repair factors. Repair foci clearly represent the recruitment and accumulation of DNA repair factors at sites of damage; however, uncertainties remain regarding their organization in the context of nuclear architecture and their biological significance. Here we identified the chromatin remodeling factor SNF2H/SMARCA5 as a novel binding partner of XRCC1, with their interaction dependent on the casein kinase 2-mediated constitutive phosphorylation of XRCC1. The proficiency of repairing H₂O₂-induced damage was strongly impaired by SNF2H knock-down, and similar impairment was observed with knock-down of both XRCC1 and SNF2H simultaneously, suggesting their role in a common repair pathway. Most SNF2H exists in the nuclear matrix fraction, forming salt extraction-resistant foci-like structures in unchallenged nuclei. Remarkably, damage-induced formation of both PAR and XRCC1 foci depended on SNF2H, and the PAR and XRCC1 foci

co-localized with the SNF2H foci. We propose a model in which a base excision repair complex containing damaged chromatin is recruited to specific locations in the nuclear matrix for repair, with this recruitment mediated by XRCC1-SNF2H interaction.

Keywords:

XRCC1; SNF2H; phosphorylation; foci; chromatin structure; nuclear matrix.

Abbreviations: AP sites, apurinic/aprimidinic sites; BER, base excision repair; CBB, Coomassie Brilliant Blue; CK2, casein kinase 2; DSB, double-strand break; OGG1, 8-oxoguanine DNA glycosylase; PAR, poly(ADP-ribose); PARP, poly(ADP-ribose) polymerase; SNF2H, sucrose non-fermenting protein 2 homolog; XRCC1, X-ray repair cross-complementing protein 1.

1. Introduction

Upon damage of chromosomal DNA, DNA repair proteins assemble at the sites of damage and execute repair reactions. There exists some controversy regarding how these repair reactions occur within the context of nuclear architecture. Some authors have proposed that damaged DNA shows little or no mobility, and that repair occurs essentially at the site of the initial damage via recruitment of a series of repair proteins *in situ* [1]. Another proposal borrows a concept from the transcription factory theory, suggesting that a portion of chromatin containing the damaged DNA is transported to specialized regions of nuclei, where repair reactions proceed [2].

The former view is supported by experiments with spatially limited irradiation, using masking filters or micro-beam [3]. These results clearly indicate minimal mobility of damaged DNA, demonstrating transport of repair proteins to the irradiated areas, where the repair reactions occur, as visualized by nucleotide analog incorporation. While these results seem to dismiss the possibility of long-range mobility of damaged chromatin within nuclei, they do not exclude the possibility of short-range movement. Despite the expectation that spatially limited irradiation would induce relatively uniform DNA damage within the irradiated area, repair protein accumulation is often not uniform [4]. This observation suggests greater repair proficiency within some parts of the irradiated area.

It is estimated that cell treatment with 10 mM H₂O₂ for 10 min induces apurinic/apyrimidinic (AP) sites on the order of 10⁴ per nucleus [5]. Under these conditions, fluorescence microscopy reveals that a number of repair protein accumulation center (often called repair foci) on the order of 10–10² per nucleus [6,7]. These estimates imply that an optically unresolved single repair focus represents the repair of dozens to hundreds of DNA damage sites, suggesting the possibility that dozens of pieces of damaged DNA are transported to a single compact region for repair. When two double-strand breaks (DSBs) are induced by restriction

nuclease expression in a nucleus, only a single focus is observed [8], strongly supporting the possibility that the two DSBs are organized into a single area of the nucleus for repair. However, it remains largely unknown what features distinguish this repair factory from other nuclei areas.

XRCC1 is an essential component of the base excision repair (BER) system. Although XRCC1 has no reported inherent enzymatic activity of its own, it interacts with a series of repair enzymes, including DNA ligase III, DNA polymerase β , poly(ADP-ribose) polymerase (PARP), AP-endonuclease, OGG1, and DNA polynucleotide kinase [9]. It has been proposed that XRCC1 acts as a dedicated scaffold of BER, organizing efficient repair reactions. It was previously thought that XRCC1 contributes to repair efficiency by stabilizing DNA ligase III. However, recent findings indicate that the interaction with DNA ligase III, or even nuclear DNA ligase III itself, is dispensable for cell survival following exposure to a DNA-damaging agent [6,10]. Thus, it remains unclear how exactly XRCC1 acts as a scaffold and coordinates DNA repair.

We previously reported that upon H₂O₂ treatment, the XRCC1 protein is transferred from the chromatin fraction to the nuclear matrix in a manner that depends on phosphorylation by casein kinase 2 (CK2) [11]. Abolishing CK2 phosphorylation dramatically reduces XRCC1 foci formation and DNA repair efficiency. One interesting possibility is that XRCC1 may assemble damaged chromatin and repair factors, and transport them to specialized repair factory areas in the nuclear matrix.

In our present study, we investigated XRCC1 translocation by screening a yeast two-hybrid library for novel XRCC1-interacting proteins. This screen identified the chromatin remodeling factor SNF2H/SMARCA5. Remarkably, SNF2H knock-down strongly impaired DNA repair proficiency as well as foci formation of both PAR and XRCC1. These results suggest that XRCC1 mediates BER complex recruitment to specific locations in the nuclear matrix.

2. Materials & methods

2.1. Yeast two-hybrid screening

Yeast two-hybrid screening of a cDNA expression library from human testis (Clontech) was conducted using a fragment of XRCC1 as bait (see RESULTS) following the manufacturer's instructions (Matchmaker; Clontech). Insert fragments of the positive clones were PCR-amplified followed by direct sequencing.

2.2. Cell culture, treatment, and immunofluorescent staining

HeLa cells were cultured as previously described [12]. For knock-down of SNF2H and XRCC1, corresponding siRNA oligonucleotides (Qiagen) were transfected at a final concentration of 10 nM for 48 hours using HiPerFect Transfection Reagent (Qiagen). The sense sequences of the utilized oligonucleotides are as follows: SNF2H, aagaggaggauagaagagcuau [13] and caauuguaugucuuuuu (Qiagen); XRCC1, ccgauggaucuacaguugca [14]; and negative control, uucuccgaacgugucacgu (Qiagen). To analyze changes in protein localization in response to DNA damage, cells were incubated with 150 μ M or 10 mM H₂O₂ [7] in fresh medium without FBS, for 10 min at 37°C. The cells were then washed twice with PBS, and incubated for 10 min in fresh medium before collection or fixation.

For immunostaining, cells grown on LabTec chamber slides (Nunc) were washed with PBS, fixed with ice-cold methanol/acetone (1:1) for 10 min and dried. The cells were then rehydrated by incubating in PBS on ice for 10 min. Chromosomal DNA and soluble/chromatin proteins were extracted *in situ* as previously described [6]. Briefly, cytosolic proteins were removed with hypotonic buffer containing 0.05% Triton X-100, chromosomal DNAs were digested with DNase I (Takara) and nuclear proteins were extracted with increasing concentrations of NaCl (0.3, 0.5, 2M). For immunostaining of γ H2AX, cells were washed with PBS and fixed in 4% paraformaldehyde in PBS, and permeabilized with blocking solution (2% skim milk, 0.2% BSA, 0.2% Triton X-100 in

PBS). Cells were incubated with primary antibody and then with Alexa 488- or Alexa 568-conjugated secondary antibody (Molecular Probes). Antibodies against hSNF2 and SNF2H were purchased from Upstate Laboratories, Inc. and Bethyl Laboratories, Inc., respectively. The utilized anti-SNF2H antibody does not cross-react with SNF2L. The anti-XRCC1 antibody was obtained from NeoMarkers (clone 33-2-5), the anti-PAR antibody from Trevigen, and anti- γ H2AX antibody from Merck Millipore. Slides were mounted in Vectashield (Vector) containing DAPI. Images were collected with an LSM510 confocal microscope using a Plan Apochromat 63 \times /1.40 oil lens (Zeiss). For quantitative analysis, cells were inoculated into 96-well plates, treated with H₂O₂, and immunostained. Images were captured using an IN Cell Analyzer 2000 (GE Health Science), and were analyzed using Developer Tool Box software (GE Health Science).

2.3. In vitro transcription and translation reaction, and template DNA construction

In vitro synthesis of XRCC1, DNA ligase III α , and SNF2H proteins was performed using the rabbit reticulocyte lysate TnT T7 Quick Coupled Transcription/Translation System (Promega), following the manufacturer's instructions. To label the synthesized proteins with biotin, biotinylated lysine-tRNA (Transcend tRNA; Promega) was added in the reaction. The template plasmid DNA for c-Myc-tagged XRCC1 has been described previously [11]. The template plasmid DNA for SNF2H or DNA ligase III α was constructed by cloning SNF2H cDNA [15] or DNA ligase III α [16] cDNA into the pGADT7 vector (Clontech), respectively. Mutant XRCC1 and SNF2H cDNA plasmids were constructed by PCR, and their sequences were confirmed.

2.4. Immunoprecipitation and western blotting

Two microliter of TnT reaction was combined with 30 μ L of 0.1% BSA in PBS, and incubated at 10 $^{\circ}$ C for 24 hours with 1 μ L of anti-mouse IgG conjugated magnetic beads (Dyna)

Biotech) to 'pre-clean' the protein mixture. This protein mixture was then combined with 0.5 μ L of anti-mouse IgG conjugated magnetic beads that were already bound with 0.1 μ g of anti-c-Myc antibody (Clontech), and incubated at 10°C for another 24 hours with constant agitation by rotary mixer (NRC-20D; Nissin Rika, Corp., Japan). The magnetic beads were then washed five times with TNE buffer (50 mM Tris-HCl, pH 8.0; 150 mM NaCl; and 1.0% NP-40), and were finally suspended in 10 μ L of SDS sample buffer. Biotin-labeled proteins in the immunoprecipitant were detected following the manufacturer's instructions (Transcend tRNA; Promega). Preparation of HeLa nuclear extracts, immunoprecipitation of cellular XRCC1 from the nuclear extracts, and western blotting procedures were performed as previously described [12]. For SNF2H immunoprecipitation, anti-SNF2H antibody was bound to anti-rabbit IgG-conjugated magnetic beads (DynaL Biotech). Anti-PCNA antibody was purchased from NeoMarkers (clone PC10), anti-LaminB antibody from Progen and anti-PARP1 antibody from R&D Systems.

2.5. Gel filtration

Gel filtration was performed as previously described [17] with slight modifications. Briefly, the HeLa nuclear extract (0.5 mg protein) was directly applied to a Superose-6 column (HR 16/50; GE Health Science) equilibrated with column running buffer (20 mM Hepes, pH 7.9; 200 mM NaCl; 1 mM DTT; 0.1 mM PMSF; and 10% glycerol). A series of 1.5-mL fraction was collected, which were then concentrated to 50 μ L using a Microcon Centrifugal Filter (YM-10; Millipore). Each concentrated fraction was analyzed by 5–20% SDS-PAGE and western blotting.

2.6. Nuclear matrix isolation

High-salt isolation of the nuclear matrix was conducted essentially as described previously [11]. After washing in PBS, cells were extracted for 3 min on ice in cytoskeleton buffer (CSK)

containing 10 mM PIPES (pH 6.8), 100 mM NaCl, 300 mM sucrose, 3 mM MgCl₂, and 1 mM EGTA, supplemented with protease inhibitor cocktail (Complete; Roche), 1 mM DTT, and 0.5% Triton X-100. The extract was centrifuged at 5000 × *g* for 3 min to separate the cytoskeletal frameworks from the soluble proteins (soluble fraction). Chromatin was solubilized by DNA digestion with 1 unit/mL of RNase-free DNase I (Takara) in CSK, for 15 min at 37°C. Total lysate volume was measured by micro pipet, and 3 volumes of 1 M ammonium sulfate in CSK were added. After 5 min on ice, the sample was centrifuged again. The supernatant was collected (chromatin fraction), and the pellet was further extracted by incubation for 5 min on ice with 2 M NaCl in CSK. The sample was centrifuged once more, and the supernatant was collected (wash). The pellet was solubilized in Reagent 3 from the ReadyPrep sequential extraction kit (BioRad) containing 5 M urea and 2 M thiourea, and this was considered the nuclear matrix-containing fraction (nuclear matrix fraction). Each fraction was aliquoted and mixed with 2 × SDS sample buffer. Samples from the soluble, chromatin, and wash fractions were heated at 95°C for 10 min prior to analysis by SDS-PAGE.

2.7. Indirect DNA repair ability assay after H₂O₂ treatment

In each well of a 96-well plate, 2000 cells were cultured and subjected to siRNA as described as above (section 2.2.). Cells were rinsed once with DMEM without FBS, and then exposed to 150 μM H₂O₂ in DMEM without FBS for 10 minutes at 37°C. The cells were next washed twice with PBS, and fresh DMEM containing FBS and the siRNA was added once again for enforcing knock-down. For Tetrazolium compound-based NAD(P)H level assay, cells were incubated for 3 or 4 hours with Cell Titer (Promega), followed by measurement of OD₄₉₀ using a plate reader (BioRad). The analyses were performed in triplicate, and two independent experiments were performed to calculate averages and standard deviations of relative NAD(P)H levels. For γH2AX assay, cells

were recovered for 1 hr in fresh medium before fixation. Nucleic γ H2AX foci were detected by immunofluorescence and the images were captured by IN Cell Analyzer 2000 (GE Health Science). Total intensity of γ H2AX foci in each nucleus was calculated by Developer Tool Box software (GE Health Science). Two independent experiments were performed to confirm reproducibility of data.

3. RESULTS

3.1. Identification of SNF2H as a novel XRCC1-interacting protein

To identify novel factors that mediate XRCC1 foci formation and/or translocation, we screened a yeast two-hybrid cDNA library prepared from human testis, where XRCC1 is abundant [18,19]. We used the BRCT2-deleted mutant XRCC1 gene as bait to avoid repeatedly obtaining positive clones with the highly represented DNA ligase III α gene, the product of which binds to XRCC1 through the BRCT2 domain [20]. Out of 1×10^8 transformants, 91 clones showed adenine and histidine prototrophy as well as β -galactosidase activity. Of these clones, 11 appeared to share the middle part of SNF2H (amino acid residues 331–531), an ATPase subunit of the ISWI chromatin remodeling complex.

3.2. Interaction between endogenous XRCC1 and SNF2H in HeLa nuclear extract

We next investigated the interaction between XRCC1 and SNF2H in HeLa nuclear extract. Endogenous XRCC1 was immunoprecipitated with anti-XRCC1 antibody, and immunoblotting was used to examine the precipitate for SNF2H and DNA ligase III α . We reproducibly detected a small amount of SNF2H (Fig. 1A). After gel filtration of the nuclear extract, we detected both XRCC1 and DNA ligase III α in the range of 220–700 kDa with a peak around 440 kDa, supporting their stable interaction (Fig. 1B). SNF2H appeared with a major peak around 4 MDa and a minor peak

around 650 kDa, coinciding with the distribution of a larger side tail of XRCC1 and DNA ligase III α (Fig. 1B). These distributions were consistent with a scenario in which part of XRCC1-Ligase III α binds to SNF2H, forming a larger ternary complex.

3.3. Regions responsible for the interaction between XRCC1 and SNF2H

To further examine the binding strength between XRCC1 and SNF2H, we conducted a co-immunoprecipitation experiment with *in vitro* translated proteins under several different salt conditions: 0.1% BSA/PBS, TNE containing 100 mM NaCl, or TNE containing 150 mM NaCl. We detected interaction between XRCC1 and Ligase III α under all tested conditions, and this interaction decreased with increasing salt concentration (Fig. 2A). In contrast, the interaction between XRCC1 and SNF2H was detected only in the 0.1% BSA/PBS condition (Fig. 2A). Interactions were not eliminated by addition of ethidium bromide, suggesting no mediation by DNA (data not shown).

We then investigated a series of deletion mutants of XRCC1 and SNF2H to determine the specific regions responsible for the interaction. Full-length SNF2H bound to the N-terminal half of XRCC1 (XRCC1-N) but not the C-terminal half (XRCC1-C1 and -C2), indicating that the two BRCT motifs located within the C-terminal half of XRCC1 (315–403 and 538–633) are not involved in the interaction with SNF2H (Fig. 2B, C). Moreover, XRCC1 bound to both the N-terminal and C-terminal truncated SNF2H mutants. Together with our above-described observations of SNF2H (331–531) interaction with XRCC1 in a yeast two-hybrid assay, these data indicate that interaction most likely occurs between the N-terminal part of XRCC1 and the middle part of SNF2H (Fig. 2C).

3.4. Increased amounts of XRCC1 and SNF2H in nuclear fraction upon H₂O₂ treatment

We previously reported that H₂O₂ treatment induces apparent translocation of chromatin-bound XRCC1 to the nuclear matrix [21]. In our present study, we investigated the behavior of SNF2H under the same condition. In non-challenged HeLa nuclear extract, SNF2H was predominantly detected in the nuclear matrix fraction, with only a small amount in the chromatin fraction (Fig. 3A). Following H₂O₂ treatment, we confirmed our previous result that XRCC1 in the NM increased compared to constitutive NM protein LaminB (Fig. 3B). SNF2H further decreased from the chromatin fraction, with a concomitant increase in the NM (Fig. 4B). PARP1 was scarcely detected in the NM in unchallenged cells, but also showed clear increase in the NM after H₂O₂ exposure, supporting the idea that DNA repair reaction is conducted in the NM. After H₂O₂ treatment, we fixed the cells, extracted chromatin proteins and DNA *in situ*, and observed them using immunofluorescence microscopy. Even in unchallenged nuclei, SNF2H appeared as foci (Fig. 3C). H₂O₂ treatment increased the fluorescence intensity without apparently changing the number of foci (Fig. 3C). XRCC1 foci were visible only after H₂O₂ treatment, and co-localized or overlapped with SNF2H foci. These observations suggest a functional link between the two proteins, and the possible involvement of SNF2H in H₂O₂-induced XRCC1 translocation.

3.5. SNF2H knock-down impaired H₂O₂-induced PAR and XRCC1 foci

DNA nicks activate PARP, which poly-ADP-ribosylates chromatin and DNA repair proteins at the sites of DNA damage. It was previously reported that XRCC1 foci formation depends on damage-induced poly-ADP-ribosylation [22]. To investigate the involvement of SNF2H in this process, we examined SNF2H localization in relation to PAR foci after H₂O₂ treatment and *in situ* extraction (Fig. 4A). Consistent with the above-described results, SNF2H foci increased their intensity in the nuclear matrix following H₂O₂ treatment without notably changing the distribution (Fig. 3, Fig. 4A). Strikingly, most of the H₂O₂-induced PAR foci co-localized with SNF2H foci (Fig.

4A). This result prompted us to propose a possibility that PAR foci formation may be dependent on SNF2H and PAR foci may form at pre-existing SNF2H foci.

To test this possibility, we examined how SNF2H knock-down influenced PAR foci formation. We found that siRNA transfection reduced the amount of SNF2H to 20% of the amount in control cells (Fig. 4B). Transfected cells also showed markedly impaired formation of extraction-resistant XRCC1 foci and PAR foci (Fig. 4C). We further quantitatively analyzed the PAR and SNF2H levels after H₂O₂ treatment in individual nuclei with or without siSNF2H transfection. Under the same exposure conditions, SNF2H knock-down led to an average decrease of 33% in the SNF2H fluorescence per nucleus, which was in accordance with the immunoblotting results (Fig. 4B, D). Compared to control siRNA-transfected cells, the siSNF2H-transfected cells also showed decreased fluorescence intensity for PAR (Fig. 4D). A correlation was also observed between PAR intensity and SNF2H intensity among siSNF2H-transfected cells ($R^2 = 0.33$), probably reflecting variation in SNF2H knock-down efficiency. These findings suggest a causal relationship between preexisting, extraction-resistant SNF2H foci and damage-induced PAR foci.

3.6. SNF2H depletion leads to diminished repair of H₂O₂-induced DNA damage

To investigate possible SNF2H involvement in repair reactions, we assayed siSNF2H-transfected cells for their proficiency in repairing H₂O₂-induced base damage. Since a decrease of cellular NAD(P)H is an indirect index of accumulation of repair intermediates [5,23], we quantified cellular NAD(P)H level to assess repair proficiency. Transfection of XRCC1 and SNF2H siRNAs reduced the respective protein levels to about 20%, as evaluated by immunoblotting (Fig. 5A). Compared to control siRNA-transfected cells, the cells transfected with siRNAs for either XRCC1 or SNF2H showed reduced NAD(P)H levels after H₂O₂ treatment (Fig. 5B). The reduction levels of NAD(P)H were comparable to previous report on H₂O₂-treated

XRCC1-null cells [24]. Simultaneous knock-down of XRCC1 and SNF2H did not further reduce the NAD(P)H level, suggesting that these proteins function in the same repair pathway (Fig. 5B). Further, we examined γ H2AX foci formation after H₂O₂ exposure [25,26]. After 10min of H₂O₂ exposure, cells were allowed to repair damage for 1 hr and remaining damage were detected by using γ H2AX assay. Compared to cells transfected with control siRNA, γ H2AX intensity was remarkably higher in cells transfected with siSNF2H or siXRCC1 (Fig. 5C, D). Combination of siSNF2H and siXRCC1 did not lead to further increase of γ H2AX intensity. This result supports the idea that SNF2H and XRCC1 are involved in the same repair pathway for H₂O₂-induced lesion.

3.7. SNF2H interacts with CK2-phosphorylated XRCC1

We previously showed that XRCC1 phosphorylation by CK2 is essential for damage-induced foci formation, and for XRCC1 translocation from chromatin to the nuclear matrix [11]. Based on this knowledge, here we investigated whether the interaction between XRCC1 and SNF2H was also dependent on phosphorylation by CK2. Immunoprecipitation analyses were performed using XRCC1-deficient EM9 cells expressing wild-type XRCC1 (WT) or mutant XRCC1 with four putative CK2 sites substituted with alanines (CKM). Electrophoretic mobility of WT protein showed a shift to cathodic side compared to CKM protein, suggesting phosphorylation of WT protein (Fig. 6) [7]. The XRCC1 mutations almost completely abolished coimmunoprecipitation with SNF2H (Fig. 6). This finding suggests that XRCC1 phosphorylation by CK2 is critical for its interaction with SNF2H, which is consistent with the involvement of SNF2H in the repair of H₂O₂-induced damage.

4. Discussion

In the present study, we identified SNF2H as a novel interacting partner of the repair scaffold protein XRCC1. In unchallenged cells, SNF2H protein mainly resides in the nuclear matrix after biochemical fractionation. With immunofluorescence microscopy, SNF2H appears as granules scattered around in the nuclei that are resistant to *in situ* extraction (Figs. 3C and 4A). On the other hand, most XRCC1 is found in the soluble chromatin fraction. Extraction-resistant insoluble XRCC1 in unchallenged cells does not show distinct sub-nuclear localization, but is rather distributed uniformly throughout the nuclei (Fig. 3C). After cells are exposed to H₂O₂, a portion of the soluble XRCC1 is redistributed to the nuclear matrix, where it forms a foci-like structure that co-localizes with the already present SNF2H foci (Fig. 3C). Importantly, damage-induced formation of both PAR foci and XRCC1 foci depends on SNF2H (Fig. 4C, D). These results support the idea that the translocation and foci formation are mediated by affinity between XRCC1 and SNF2H.

We previously demonstrated that XRCC1 in the chromatin fraction is constitutively phosphorylated by CK2, and that this phosphorylated form is likely to translocate to the nuclear matrix following H₂O₂ treatment [11]. Consistently, our present results showed that wild-type XRCC1 interacted with SNF2H, while the non-phosphorylatable mutant XRCC1 (CKM) did not (Fig. 6). We currently have few clues indicating how this interaction is regulated in a damage-dependent manner. The relatively weak binary interaction that we observed between XRCC1 and SNF2H (Fig. 1A, Fig. 2A) may be explained by the absence of damage-inducible components, such as PAR. Since previous findings establish that XRCC1 foci formation is absolutely dependent on PAR [22,27], it is reasonable to speculate PAR affects the interaction between XRCC1 and SNF2H.

SNF2H knock-down also compromised efficient repair reactions, suggesting a functional importance of its interaction with XRCC1 (Fig. 5). Our present study did not examine how the chromatin remodeling activity of SNF2H contributes to DNA repair reactions. Chromatin

remodeling/histone chaperoning by SWI/SNF, INO80, and CAF-I have been implicated in double-strand break repair and nucleotide excision repair [28-30]. Previous work also shows that nucleosome structure has an inhibitory effect on BER [31,32], thus requiring remodeling prior to repair. Interestingly, simultaneous knock-down of XRCC1 and SNF2H did not significantly increase the repair defect compared with knock-down of either alone. This may imply that the major, if not only, function of XRCC1 is to couple repair reactions with the remodeling of damaged chromatin.

Odell et al demonstrated that *in vitro* repair of nucleosomal DNA requires a high concentration of DNA ligase III-XRCC1 complex [33], indicating that this is the rate-limiting step of the BER reaction in chromosomal DNA. Another report showed that XRCC1 and PARP are recruited specifically to sites of DNA damage in heterochromatin [34], and that XRCC1 recruitment to heterochromatin depends on PARP activity. PARP may function as a nick sensor, and may also contribute to chromatin structure remodeling [35,36]. Repair reactions in the heterochromatin require extensive disruption of chromatin structure. Furthermore, after completion of ligation, chromosomal DNA must be restored into heterochromatin. In cases where epigenetic information is recovered after repair of base damage, SNF2H and its interacting partner, DNMT1 [37], may contribute to this restoration. Thus, efficient and controlled BER reactions in the higher chromosomal structure are executed by interactions between XRCC1 and its partner proteins. This exciting possibility should be explored in future studies.

In conclusion, our results indicate that phosphorylated XRCC1 interacts with SNF2H. This interaction is responsible for the foci formation of XRCC1 in the nuclear matrix and efficient repair of H₂O₂-induced damage in chromosomal DNA.

Conflict of interest statement

None declared.

Acknowledgements

The cDNA plasmids of DNA ligase III α and SNF2H were kindly provided by Dr. D. Barnes and Dr. Y. Nakamura, respectively.

Funding

This work was supported by the JSPS KAKENHI (Grant Number 22510206 to Y.K.).

Figure legends

Fig. 1. XRCC1 interacts with SNF2H in HeLa nuclear extracts. (A) HeLa nuclear extracts were immunoprecipitated (IP) with or without anti-XRCC1 antibody, and the precipitates were analyzed by western blotting (WB) using antibodies against XRCC1, SNF2H, and DNA ligase III α . (B) Nuclear extracts were prepared from HeLa cells overexpressing XRCC1, and applied to a Superrose-6 HR column equilibrated with the column running buffer (20 mM Hepes, pH 7.9; 200 mM NaCl; 1 mM DTT; 0.1 mM PMSF; and 10% glycerol). Fractions were collected and analyzed by SDS-PAGE followed by western blotting. The fraction numbers are indicated at the top. The fractions corresponding to proteins of known molecular mass are indicated in kilodaltons below the figure. The void volume of the column is marked as void.

Fig. 2. The N-terminal region of XRCC1 interacts with the middle region of SNF2H. (A) Myc-tagged XRCC1, SNF2H, and DNA ligase III α were produced by an *in vitro* TnT system and labeled with biotin. These TnT products were mixed, and myc-XRCC1 was immunoprecipitated with or without anti-myc antibody (IP, + α myc or - α myc). The binding affinity of the proteins was determined under three incubation conditions: PBS containing 0.1% BSA, TNE buffer containing 100 mM NaCl, and TNE buffer containing 150 mM NaCl. Precipitates were washed with TNE buffer containing 50 mM NaCl, and analyzed with SDS-PAGE. (B) To determine the protein regions responsible for the interaction, the *in vitro* TnT system was used to produce full-length proteins (FL), and N-terminal (N) or C-terminal (C) regions of the proteins. These products were subjected to co-immunoprecipitation analysis. Arrowheads indicate SNF2H variants and open arrowheads indicate XRCC1 variants. (C) Schematic illustration of the truncated mutant proteins. Numbers indicate the corresponding numbers of amino acids. The Y2H fragment of SNF2H corresponds to the polypeptides found in positive clones in the yeast 2-hybrid screening. Gray boxes indicate the region of each protein responsible for the interaction.

Fig. 3. H₂O₂ treatment led to increased XRCC1 and SNF2H in the nuclear matrix. (A) HeLa cellular proteins were sequentially extracted into the following fractions: soluble (Sol), chromatin (Ch), wash (W), and nuclear matrix (NM). Each fraction was analyzed with SDS-PAGE followed by western blotting using the indicated antibodies. The Sol, Ch, W, and NM lanes contain proteins corresponding to 0.5×10^6 , 0.5×10^6 , 1×10^6 , and 1×10^6 cells, respectively. Arrowheads indicate histones detected by CBB staining of the SDS polyacrylamide gel. (B) HeLa cells were treated with H₂O₂ and protein fractions were collected and analyzed as described in the panel A. Numbers indicate fold increase of the band intensity of nuclear matrix fractions (NM) after H₂O₂ treatment. The mean \pm standard deviation of two experiments is shown. (C) Cells were treated with 10 mM

H₂O₂ for 10 min. After *in situ* extraction of chromosomal DNA and soluble/chromatin proteins, SNF2H and XRCC1 were detected in the nuclear matrix using specific antibodies. Plot profile of the fluorescence intensities of SNF2H and XRCC1 were generated through the indicated lines in the image.

Fig. 4. After H₂O₂ treatment, XRCC1 and PAR foci formation was associated with SNF2H foci in the nuclear matrix. (A) HeLa cells were treated with H₂O₂ as shown in Fig. 3C, then DNA and soluble proteins were extracted *in situ*. PAR and SNF2H in the nuclear matrix were immunostained with specific antibodies. (B) In HeLa cells, SNF2H was knocked-down by introduction of specific siRNA (SNF), but not by non-specific siRNA (Cont.). CBB staining of the membrane used for western detection is shown. (C) SNF2H knocked-down cells were exposed to H₂O₂ and immunostained with anti-SNF2H, -XRCC1, or -PAR antibodies. The cell surrounded by arrowheads exhibited SNF2H knock-down. (D) HeLa cells were inoculated into 96 well plates, and SNF2H was knocked-down as shown in panel B. The cells were treated with H₂O₂, and PAR and SNF2H foci in the nuclear matrix were stained with specific antibodies. Images were collected, and the relative intensities of signals in each nucleus were measured and plotted. Magenta and blue spots correspond to the nuclei of cells transfected with control siRNA and SNF2H siRNA, respectively.

Fig. 5. SNF2H depletion led to reduced DNA repair activity in HeLa cells. (A) Cells were transfected with siRNA of negative control (NC), SNF2H (SN), and XRCC1 (XR) alone, or with a combination of SN and XR. Two different siRNAs (SN-1 and -2) were used for SNF2H knock-down. (B) HeLa cells were transfected with siRNA for 48 hours before 150 μ M H₂O₂ treatment. After 10 min of H₂O₂ treatment, cells were rinsed and incubated for 3 to 4 hours with

fresh medium containing the corresponding siRNA and the tetrazolium compound. The absorbance at 490 nm of the cells transfected with negative control (NC) siRNA was plotted as a relative NAD(P)H level of 1.0. The mean \pm standard deviation of two experiments is shown. (C, D) HeLa cells were transfected with siRNA and incubated in medium containing 150 μ M (C) or 0 μ M (D) H₂O₂ as shown in panel B. After rinse, cells were incubated in fresh medium for 1 hr and fixed with paraformaldehyde. γ H2AX foci were detected with specific antibody (red). DNA was detected with DAPI (blue).

Fig. 6. The interaction between XRCC1 and SNF2H depends on phosphorylation of XRCC1 by CK2. Immunoprecipitation was performed with prepared nuclear extracts from XRCC1-deficient EM9 cells harboring expression vector only (Vec), wild-type XRCC1 cDNA (WT), and mutant XRCC1 cDNA that is not phosphorylated by CK2 (CKM). SNF2H was immunoprecipitated with (+) or without (–) anti-SNF2H antibody. The precipitates were separated and analyzed with western blotting (WB) using anti-SNF2H or anti-XRCC1 antibodies.

References

- [1] M. Volker, M.J. Moné, P. Karmakar, A. van Hoffen, W. Schul, W. Vermeulen, et al., Sequential assembly of the nucleotide excision repair factors in vivo, *Mol Cell*. 8 (2001) 213–224.
- [2] P. Meister, Nuclear factories for signalling and repairing DNA double strand breaks in living fission yeast, *Nucleic Acids Res*. 31 (2003) 5064–5073. doi:10.1093/nar/gkg719.
- [3] B.E. Nelms, R.S. Maser, J.F. MacKay, M.G. Lagally, J.H. Petrini, In situ visualization of DNA double-strand break repair in human fibroblasts, *Science*. 280 (1998) 590–592.
- [4] V. Hable, G.A. Drexler, T. Brüning, C. Burgdorf, C. Greubel, A. Derer, et al., Recruitment Kinetics of DNA Repair Proteins Mdc1 and Rad52 but Not 53BP1 Depend on Damage Complexity, *PLoS ONE*. 7 (2012) e41943–11. doi:10.1371/journal.pone.0041943.

- [5] J. Nakamura, V.E. Walker, P.B. Upton, S.Y. Chiang, Y.W. Kow, J.A. Swenberg, Highly sensitive apurinic/apyrimidinic site assay can detect spontaneous and chemically induced depurination under physiological conditions, *Cancer Res.* 58 (1998) 222–225.
- [6] Y. Kubota, S. Horiuchi, Independent roles of XRCC1's two BRCT motifs in recovery from methylation damage, *DNA Repair (Amst)*. 2 (2003) 407–415.
- [7] J.I. Loizou, S.F. El-Khamisy, A. Zlatanou, D.J. Moore, D.W. Chan, J. Qin, et al., The protein kinase CK2 facilitates repair of chromosomal DNA single-strand breaks, *Cell*. 117 (2004) 17–28.
- [8] M. Lisby, U.H. Mortensen, R. Rothstein, Colocalization of multiple DNA double-strand breaks at a single Rad52 repair centre, *Nat Cell Biol.* 5 (2003) 572–577. doi:10.1038/ncb997.
- [9] K.W. Caldecott, XRCC1 and DNA strand break repair, *DNA Repair (Amst)*. 2 (2003) 955–969.
- [10] Y. Gao, S. Katyal, Y. Lee, J. Zhao, J.E. Rehg, H.R. Russell, et al., DNA ligase III is critical for mtDNA integrity but not Xrcc1-mediated nuclear DNA repair, *Nature*. 471 (2011) 240–244. doi:10.1038/nature09773.
- [11] Y. Kubota, T. Takanami, A. Higashitani, S. Horiuchi, Localization of X-ray cross complementing gene 1 protein in the nuclear matrix is controlled by casein kinase II-dependent phosphorylation in response to oxidative damage, *DNA Repair (Amst)*. 8 (2009) 953–960. doi:10.1016/j.dnarep.2009.06.003.
- [12] T. Takanami, J. Nakamura, Y. Kubota, S. Horiuchi, The Arg280His polymorphism in X-ray repair cross-complementing gene 1 impairs DNA repair ability, *582* (2005) 135–145. doi:10.1016/j.mrgentox.2005.01.007.
- [13] N. Collins, R.A. Poot, I. Kukimoto, C. García-Jiménez, G. Dellaire, P.D. Varga-Weisz, An ACF1-ISWI chromatin-remodeling complex is required for DNA replication through heterochromatin, *Nat Genet.* 32 (2002) 627–632. doi:10.1038/ng1046.
- [14] J.T. Heale, A.R. Ball, J.A. Schmiesing, J.-S. Kim, X. Kong, S. Zhou, et al., Condensin I interacts with the PARP-1-XRCC1 complex and functions in DNA single-strand break repair, *Mol Cell*. 21 (2006) 837–848. doi:10.1016/j.molcel.2006.01.036.
- [15] T. Aihara, Y. Miyoshi, K. Koyama, M. Suzuki, E. Takahashi, M. Monden, et al., Cloning and mapping of SMARCA5 encoding hSNF2H, a novel human homologue of Drosophila ISWI, *Cytogenet Cell Genet.* 81 (1998) 191–193.
- [16] Y.F. Wei, P. Robins, K. Carter, K. Caldecott, D.J. Pappin, G.L. Yu, et al., Molecular cloning and expression of human cDNAs encoding a novel DNA ligase IV and DNA ligase III, an enzyme active in DNA repair and recombination, *Mol Cell Biol.* 15 (1995) 3206–3216.
- [17] A.R. Meetei, S. Sechi, M. Wallisch, D. Yang, M.K. Young, H. Joenje, et al., A multiprotein nuclear complex connects Fanconi anemia and Bloom syndrome, *Mol Cell Biol.* 23 (2003) 3417–3426.
- [18] Z.Q. Zhou, C.A. Walter, Expression of the DNA repair gene XRCC1 in baboon tissues, *Mutat. Res.* 348 (1995) 111–116.
- [19] R. Petryszak, T. Burdett, B. Fiorelli, N.A. Fonseca, M. Gonzalez-Porta, E. Hastings, et al., Expression Atlas update--a database of gene and transcript expression from microarray- and sequencing-based functional genomics experiments, *Nucleic Acids Res.* 42 (2014) D926–32. doi:10.1093/nar/gkt1270.

- [20] K.W. Caldecott, C.K. McKeown, J.D. Tucker, S. Ljungquist, L.H. Thompson, An interaction between the mammalian DNA repair protein XRCC1 and DNA ligase III, *Mol Cell Biol.* 14 (1994) 68–76.
- [21] Y. Kubota, T. Takanami, A. Higashitani, S. Horiuchi, Localization of X-ray cross complementing gene 1 protein in the nuclear matrix is controlled by casein kinase II-dependent phosphorylation in response to oxidative damage, *DNA Repair (Amst)*. 8 (2009) 953–960. doi:10.1016/j.dnarep.2009.06.003.
- [22] S.F. El-Khamisy, M. Masutani, H. Suzuki, K.W. Caldecott, A requirement for PARP-1 for the assembly or stability of XRCC1 nuclear foci at sites of oxidative DNA damage, *Nucleic Acids Res.* 31 (2003) 5526–5533.
- [23] B.F. Pachkowski, S. Winkel, Y. Kubota, J.A. Swenberg, R.C. Millikan, J. Nakamura, XRCC1 genotype and breast cancer: functional studies and epidemiologic data show interactions between XRCC1 codon 280 His and smoking, *Cancer Res.* 66 (2006) 2860–2868. doi:10.1158/0008-5472.CAN-05-3388.
- [24] B.F. Pachkowski, XRCC1 Genotype and Breast Cancer: Functional Studies and Epidemiologic Data Show Interactions between XRCC1 Codon 280 His and Smoking, *Cancer Res.* 66 (2006) 2860–2868. doi:10.1158/0008-5472.CAN-05-3388.
- [25] T. Katsube, M. Mori, H. Tsuji, T. Shiomi, B. Wang, Q. Liu, et al., Most hydrogen peroxide-induced histone H2AX phosphorylation is mediated by ATR and is not dependent on DNA double-strand breaks, *Journal of Biochemistry.* 156 (2014) 85–95. doi:10.1093/jb/mvu021.
- [26] J.K. Horton, D.F. Stefanick, R. Prasad, N.R. Gassman, P.S. Kedar, S.H. Wilson, Base excision repair defects invoke hypersensitivity to PARP inhibition, *Mol. Cancer Res.* 12 (2014) 1128–1139. doi:10.1158/1541-7786.MCR-13-0502.
- [27] C. Breslin, P. Hornyak, A. Ridley, S.L. Rulten, H. Hanzlikova, A.W. Oliver, et al., The XRCC1 phosphate-binding pocket binds poly (ADP-ribose) and is required for XRCC1 function, *Nucleic Acids Res.* 43 (2015) 6934–6944. doi:10.1093/nar/gkv623.
- [28] J.-H. Park, E.J. Park, H.-S. Lee, S.-J. Kim, S.K. Hur, A.N. Imbalzano, et al., Mammalian SWI/SNF complexes facilitate DNA double-strand break repair by promoting gamma-H2AX induction, *Embo J.* 25 (2006) 3986–3997. doi:10.1038/sj.emboj.7601291.
- [29] F.R. Neumann, V. Dion, L.R. Gehlen, M. Tsai-Pflugfelder, R. Schmid, A. Taddei, et al., Targeted INO80 enhances subnuclear chromatin movement and ectopic homologous recombination, *Genes Dev.* 26 (2012) 369–383. doi:10.1101/gad.176156.111.
- [30] J.A. Mello, H.H.W. Silljé, D.M.J. Roche, D.B. Kirschner, E.A. Nigg, G. Almouzni, Human Asf1 and CAF-1 interact and synergize in a repair-coupled nucleosome assembly pathway, *EMBO Rep.* 3 (2002) 329–334. doi:10.1093/embo-reports/kvf068.
- [31] B.C. Beard, S.H. Wilson, M.J. Smerdon, Suppressed catalytic activity of base excision repair enzymes on rotationally positioned uracil in nucleosomes, *Proc Natl Acad Sci USA.* 100 (2003) 7465–7470. doi:10.1073/pnas.1330328100.
- [32] A.K. Hinz, Y. Wang, M.J. Smerdon, Base Excision Repair in a Glucocorticoid Response Element: EFFECT OF GLUCOCORTICOID RECEPTOR BINDING, *J Biol Chem.* 285 (2010) 28683–28690. doi:10.1074/jbc.M110.113530.
- [33] I.D. Odell, J.E. Barbour, D.L. Murphy, J.A. Della-Maria, J.B. Sweasy, A.E. Tomkinson, et al., Nucleosome Disruption by DNA Ligase III-XRCC1 Promotes Efficient Base Excision Repair, *Mol Cell Biol.* 31 (2011) 4623–4632. doi:10.1128/MCB.05715-11.
- [34] L. Lan, S. Nakajima, L. Wei, L. Sun, C.L. Hsieh, R.W. Sobol, et al., Novel method for site-specific induction of oxidative DNA damage reveals differences in recruitment of

- repair proteins to heterochromatin and euchromatin, *Nucleic Acids Res.* 42 (2014) 2330–2345. doi:10.1093/nar/gkt1233.
- [35] G.G. Poirier, G. de Murcia, J. Jongstra-Bilen, C. Niedergang, P. Mandel, Poly(ADP-ribosyl)ation of polynucleosomes causes relaxation of chromatin structure, *Proc Natl Acad Sci USA.* 79 (1982) 3423–3427.
- [36] C.A. Realini, F.R. Althaus, Histone shuttling by poly(ADP-ribosylation), *J Biol Chem.* 267 (1992) 18858–18865.
- [37] A.K. Robertson, T.M. Geiman, U.T. Sankpal, G.L. Hager, K.D. Robertson, Effects of chromatin structure on the enzymatic and DNA binding functions of DNA methyltransferases DNMT1 and Dnmt3a in vitro, *Biochemical and Biophysical Research Communications.* 322 (2004) 110–118. doi:10.1016/j.bbrc.2004.07.083.

Figure 1

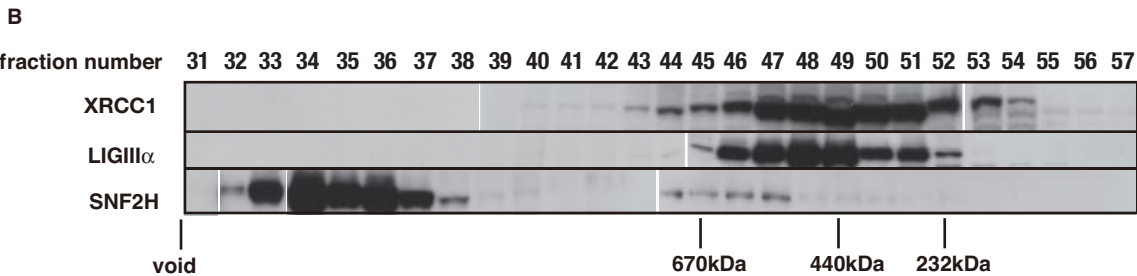
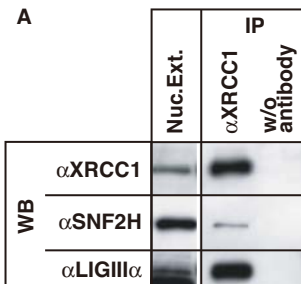
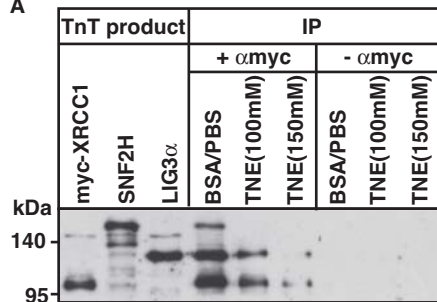
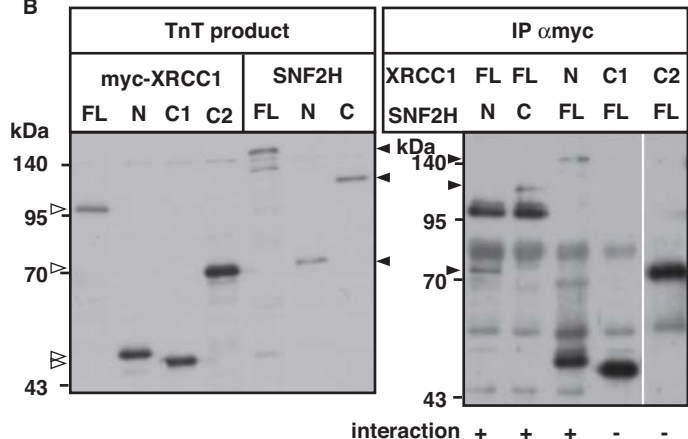


Figure 2

A



B



C

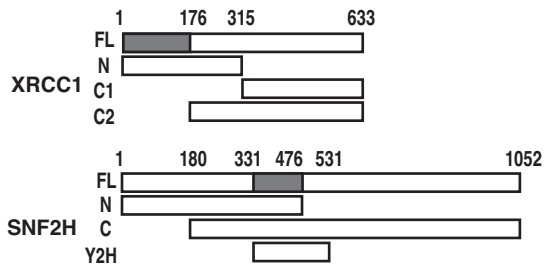


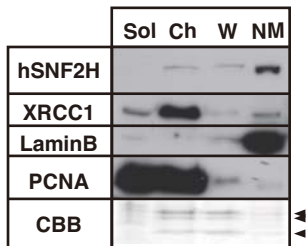
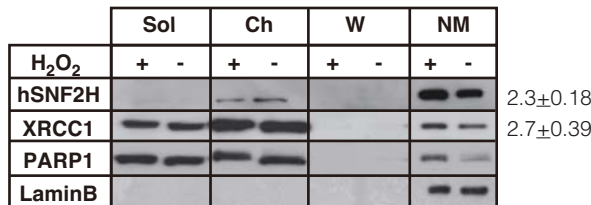
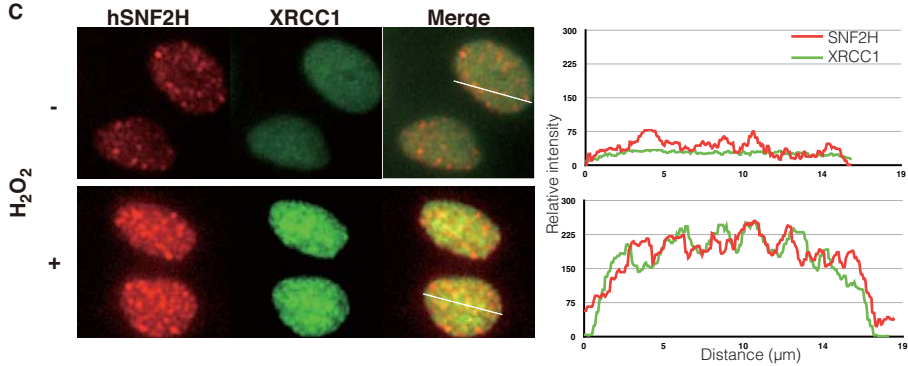
Figure 3**A****B****C**

Figure 4

A

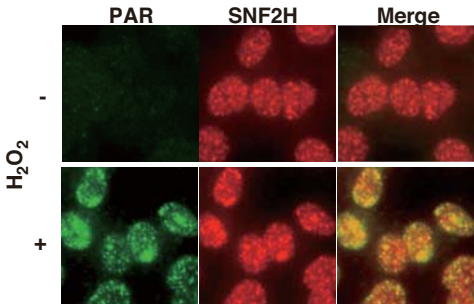
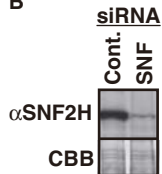
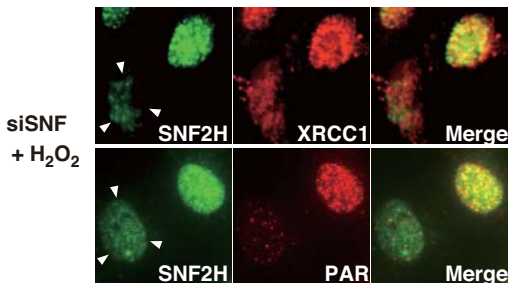


Figure 4

B



C



D

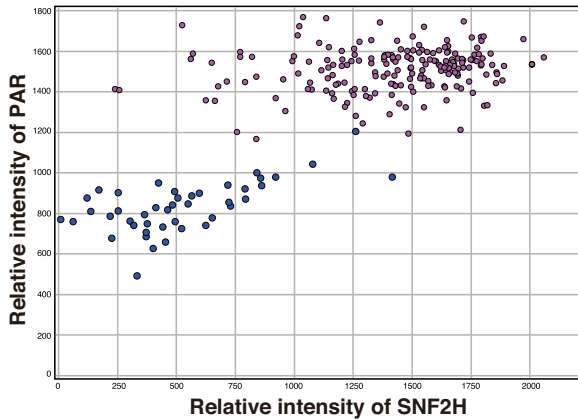
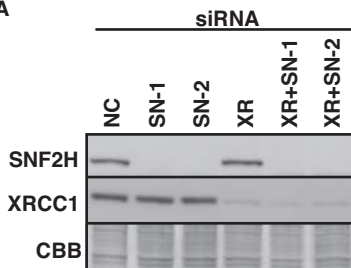


Figure 5

A



B

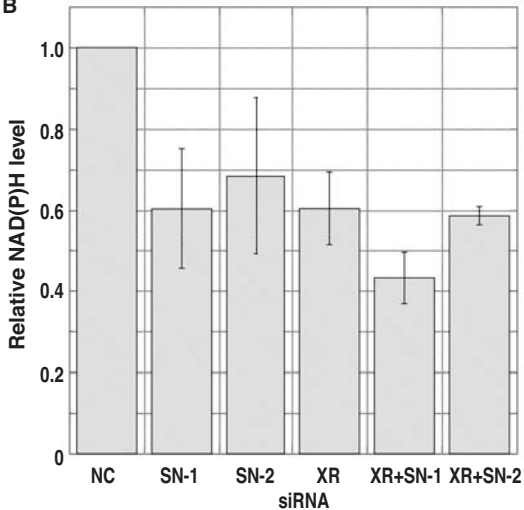


Figure 5C

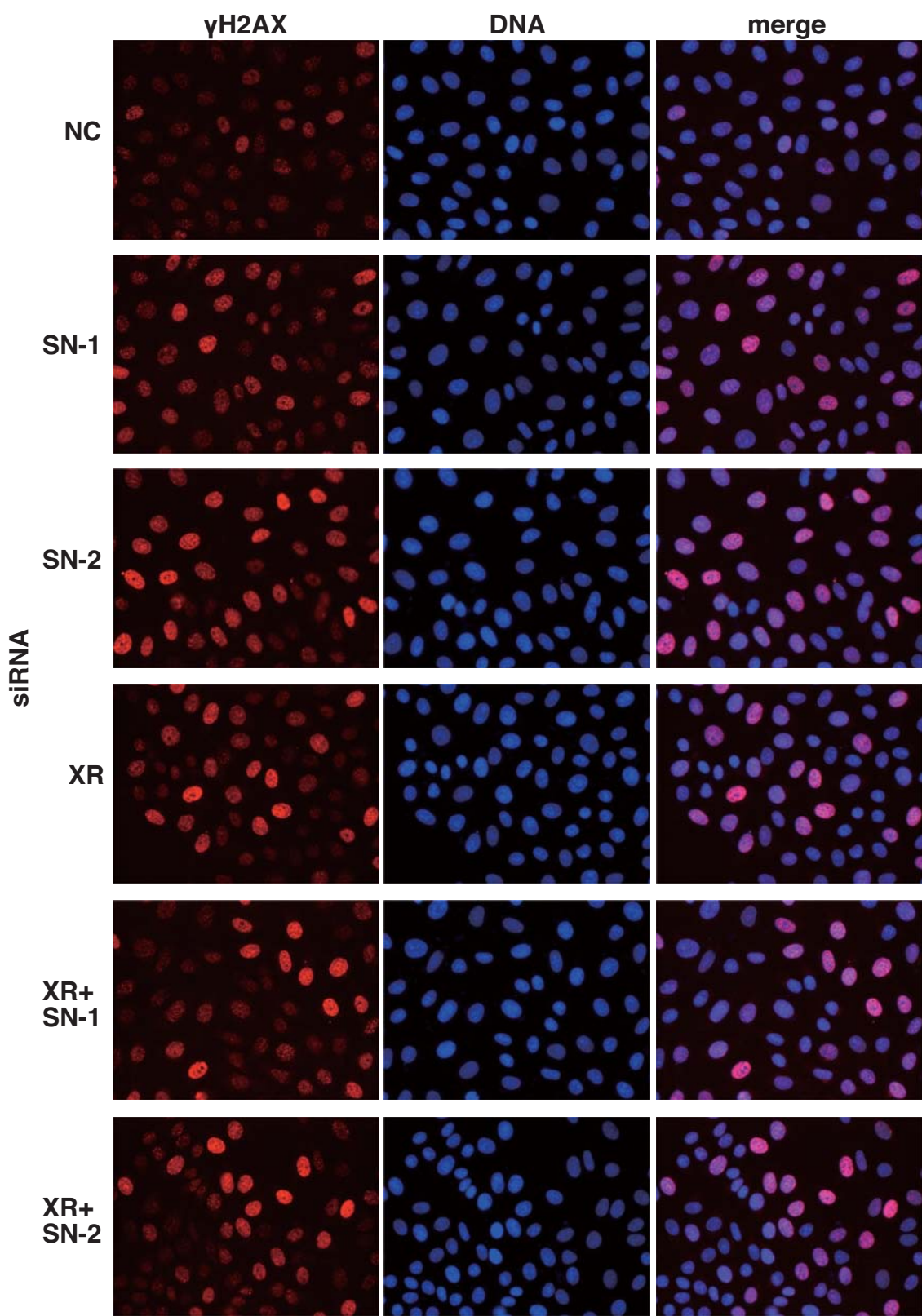


Figure 5D

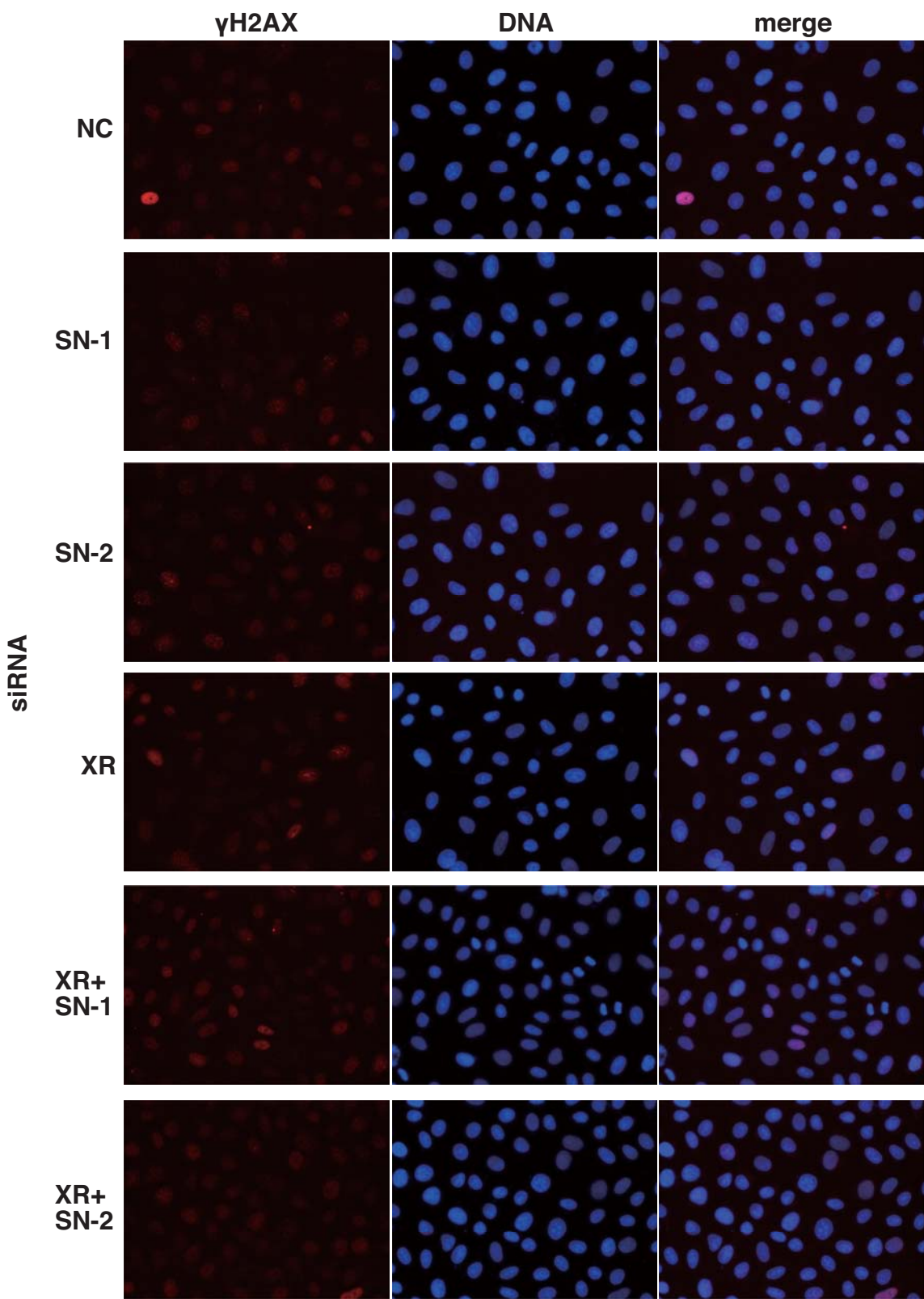


Figure 6